Brain Structure, Connectivity, and Cognitive Changes Following Revascularization Surgery in Adult Moyamoya Disease

Ken Kazumata, MD, PhD*
Khin Khin Tha, MD, PhD‡
Kikutaro Tokairin, MD*
Masaki Ito, MD, PhD*
Haruto Uchino, MD*
Masahito Kawabori, MD, PhD*
Taku Sugiyama, MD, PhD*

*Department of Neurosurgery, Hokkaido University Graduate School of Medicine, Japan; ‡Department of Diagnostic and Interventional Radiology, Hokkaido University Hospital, Japan

Correspondence:
Ken Kazumata, MD,
Department of Neurosurgery,
Hokkaido University Graduate School of Medicine,
North 15 West 7, Kita,
Sapporo 060–8638, Japan.
Email: kazumata@med.hokudai.ac.jp

Received, October 23, 2018.
Accepted, January 23, 2019.

BACKGROUND: The effect of the combined direct/indirect revascularization surgery in Moyamoya disease has not been evaluated sufficiently with regard to cognitive function, brain microstructure, and connectivity.

OBJECTIVE: To investigate structural and functional changes following revascularization surgery in patients with moyamoya disease (MMD) through a combined analysis of brain morphology, microstructure, connectivity, and neurobehavioral data.

METHODS: Neurobehavioral and neuroimaging examinations were performed in 25 adults with MMD prior to and >12 mo after revascularization surgery. Cognitive function was investigated using the Wechsler Adult Intelligence Scale-III, Trail-Making Test, Wisconsin Card Sorting Test, Continuous Performance Test, Stroop test, and Wechsler Memory Scale. We assessed white matter integrity using diffusion tensor imaging, brain morphometry using magnetization-prepared rapid gradient-echo sequences, and brain connectivity using resting-state functional magnetic resonance imaging (MRI).

RESULTS: Cognitive examinations revealed significant changes in the full-scale intelligence quotient (IQ), performance IQ (PIQ), perceptual organization (PO), processing speed, and Stroop test scores after surgery ($P < .05$). Enlargement of the lateral ventricle, volume reductions in the corpus callosum and subcortical nuclei, and cortical thinning in the prefrontal cortex were also observed ($P < .05$). Fractional anisotropy in the white matter tracts, including the superior longitudinal fasciculus, increased 2 to 4 yr after surgery, relative to that observed in the presurgical state ($P < .05$). Resting-state brain connectivity was increased predominantly in the fronto-cerebellar circuit and was positively correlated with improvements in PIQ and PO ($P < .05$).

CONCLUSION: Revascularization surgery may improve processing speed and attention in adult patients with MMD. Further, multimodal MRI may be useful for detecting subtle postsurgical brain structural changes, reorganization of white matter tracts, and brain connectivity alterations.

KEY WORDS: Cerebrovascular disorders, Cognitive function, EC-IC bypass, Intracranial artery disease, Moyamoya disease

Neurosurgery 0:1–10, 2019 DOI:10.1093/neuros/nyz176 www.neurosurgery-online.com

Moyamoya disease (MMD) is a rare cerebrovascular disorder involving noninflammatory occlusive changes of the intracranial internal carotid artery. Its angiographical appearance is characterized by enlarged basal perforating arteries resembling a puff of smoke.[1] While progressive vascular lesions are known to induce cerebral ischemia in children, adult patients occasionally lack focal ischemic symptoms due to hemodynamic compensation. However, previous studies have indicated that persistent ischemia in the frontal lobe can impair executive function, attention, and working memory (WM).[2-4]

Clinicians have expressed increasing interest in whether cognitive dysfunction is reversible in patients with MMD, and whether revascularization surgery can improve cognitive outcomes.[5] Despite the potential benefits of surgery, there is a risk of cognitive deterioration due to surgery-related factors including general anesthesia, perioperative stroke,

procedure-related brain injury, and postoperative cerebral hyperperfusion. Therefore, cognitive outcomes are clinically relevant, particularly in adults, as patients may be concerned about job performance and education postsurgery. Recent studies have reported that short-term cognitive outcomes remain unchanged at 6 mo following revascularization surgery.[6] However, information is still limited regarding patients' cognitive outcomes following the procedure.

Neuroimaging examinations are important for assessing brain structure and function, particularly brain morphometry, which enables the detection of localized brain atrophy. Advances in magnetic resonance imaging (MRI) acquisition, including diffusion tensor imaging (DTI), postacquisition image processing techniques, and quantification of diffusion parameters, have also enabled researchers and clinicians to determine the white matter injury profile (eg, reduced fiber density, demyelination, axonal injury).[7] Resting-state functional MRI (rs-fMRI) can measure low-frequency blood-oxygen-level dependent (BOLD) fluctuations, allowing researchers to estimate brain connectivity across distant regions.[8,9] Furthermore, postprocessing of neuroimaging data involving registration to a common space enables semi-automatic longitudinal evaluation, permitting the detection of subtle postoperative changes in the brain.[10] Thus, combining multimodal MRI approaches with behavioral measures of cognitive function may help to elucidate the mechanisms underlying postoperative alterations in brain structure and function in patients with MMD.

In the present study, we investigated alterations in cognitive performance and neuroimaging findings in patients with MMD after vs before revascularization surgery. The white matter integrity, brain morphometry, and functional connectivity were assessed using DTI, magnetization-prepared rapid gradient-echo (MPRAGE) sequences, and rs-fMRI, respectively. The present study also explored interactions among the regional brain atrophy, microstructural changes in white matter, resting brain connectivity, and cognitive outcomes.

ABBREVIATIONS: BOLD, blood-oxygen-level dependent; **CSF,** cerebrospinal fluid; **DTI,** diffusion tensor imaging; **FA,** fractional anisotropy; **FDR,** false discovery rate; **FIQ,** full-scale intelligence quotient; **IQ,** intelligence quotient; **MD,** mean diffusivity; **MMD,** moyamoya disease; **MPRAGE,** magnetization-prepared rapid gradient-echo; **MRI,** magnetic resonance imaging; **PIQ,** performance IQ; **PO,** perceptual organization; **PS,** processing speed; **rCBF,** regional cerebral blood flow; **ROI,** region of interest; **rs-MRI,** resting-state functional MRI; **SLF,** superior longitudinal fasciculus; **TBSS,** tract-based spatial statistics; **TFCE,** threshold-free cluster enhancement; **TMT,** Trail-Making Test; **VIQ,** verbal intelligence quotient; **WAIS-III,** Wechsler Adult Intelligence Scale version III; **WCST,** Wisconsin Card Sorting Test; **WM,** working memory; **WMS,** Wechsler Memory Scale

Supplemental digital content is available for this article at www.neurosurgeryonline.com.

METHODS

This prospective study was approved by the Research Ethics Committee of our hospital. Written informed consent was obtained from all participants.

Patients

Clinical diagnoses of MMD were made in accordance with the consensus criteria and guidelines for MMD proposed by the Research Committee on Spontaneous Occlusion of the Circle of Willis.[1] The study included 25 consecutive adult patients with MMD (5 men, 20 women; age range: 19-53 yr; mean age: 37.6 ± 9.7 yr) who were treated at our hospital between January 2013 and March 2017. None of the included patients exhibited neurological deficits due to stroke or psychiatric illness at the time of inclusion. Patients with perioperative stroke complications that would hinder multimodal neuroimaging analysis were excluded. Among the 25 included patients, 3 did not complete the follow-up neuropsychological evaluations. For the surgical procedures, we performed double superficial temporal artery-middle cerebral artery anastomosis and encephalo-duro-myo-arterio-pericranial-synangiosis.[11,12] The surgical procedures and postoperative management methods are described in detail elsewhere.[11] Detailed descriptions of the surgical indications are provided in **Supplemental Digital Content 1.**

Study Protocol and Image Acquisition

Patients underwent neuropsychological examinations prior to and >12 mo after surgery (average: 21.2 ± 9.1 mo, range: 12-44 mo). Cerebral perfusion was evaluated preoperatively. Multimodal MRI was used to assess white matter microstructure, gray/white matter morphometry, and resting brain connectivity at baseline and during the postoperative period. Detailed descriptions of the neuroimaging parameters, cognitive evaluations, and analysis methods are provided in **Supplemental Digital Content 1.**

Cognitive Performance Measurements

The intelligence quotient was assessed using the Wechsler Adult Intelligence Scale version III (WAIS-III). In addition to the full-scale intelligence quotient (FIQ), performance intelligence quotient (PIQ), and verbal intelligence quotient (VIQ), 4 underlying index scores were assessed, namely verbal comprehension, perceptual organization (PO), WM, and processing speed (PS). We also utilized a neuropsychological battery sensitive to frontal lobe dysfunction comprising the Wisconsin Card Sorting Test (WCST), Trail-Making Test (TMT, parts A and B), Continuous Performance Test, and Stroop test. The Wechsler Memory Scale (WMS-R), Third Edition, was used to examine memory function. All neurobehavioral examinations were performed over ~2 d.

Assessment of Preoperative Cerebral Perfusion

Regional cerebral blood flow (rCBF) values were measured using [123I] N-isopropyl p-iodoamphetamine/single photon emission computed tomography. Images were normalized to the standard template in Statistical Parametric Mapping version 12 (SPM12, Wellcome Department of Cognitive Neurology, University College London, London, United Kingdom; www.fil.ion.ucl.ac.uk/spm/).[13] Regions of interest (ROIs) in the lateral prefrontal, medial frontal, and parietal cortices were normalized to the average CBF in the cerebellar hemisphere.

Identification of Morphometric Alterations in the Brain

T1-MPRAGE images were segmented using the FreeSurfer (version 5.1.0; surfer.nmr.mgh.harvard.edu) default automated gyral-based parcellation method, yielding a total of 150 regional parameters.[14] Brain morphometric measurements included ventricle volume, cortical/subcortical gray and white matter volume, and cortical thickness. Default longitudinal processing was used for image co-registration to create a template for each participant (https://surfer.nmr.mgh.harvard.edu/fswiki/LongitudinalProcessing).[15]

Identification of Microstructural Alterations in the White Matter

The diffusion imaging data were processed using FSL (http://fsl.fmrib.ox.ac.uk/fsl/fslwiki/).[16] Fractional anisotropy (FA) and mean diffusivity (MD) were extracted using default parameters in FSL. Differences in the major DTI indices between the baseline and postsurgical images were then examined using tract-based spatial statistics (TBSS), which is a component of FSL. The results were corrected for multiple comparisons across space using threshold-free cluster enhancement (TFCE). Image co-registration was performed via transformation to FMRIB58_FA standard space, as the target in TBSS. For the 2 major DTI indices (ie, FA and MD), we calculated the mean value and number of voxels reaching statistical significance ($P < .05$, TFCE corrected). An ROI-based analysis was also performed to extract the DTI parameters from the images in the standardized space. ROIs were defined using the JHU white matter atlas available in FSL.[17]

Identification of Resting Brain Connectivity Using rs-fMRI

The CONN toolbox (Conn version 18, http://www.alfnie.com/software) was used to perform seed-based analyses by computing the temporal correlations between the BOLD signals from a given ROI and those of all other ROIs in the brain. ROIs were placed using the automated anatomic labeling atlas available in the CONN plug-in. Pearson correlations for all time-course pairs were computed for each participant and transformed into z-scores via Fisher's transformation (see **Supplemental Digital Content 1** for detailed methods).

Data Analysis

Preoperative and postoperative cognitive test results (IQ, TMT-A, B, WCST, Stroop test, Continuous Performance Test, WMS-R) were compared using paired *t*-tests. The TMT-A and TMT-B scores were transformed to z-scores, while the number of categorical errors was determined for the WCST. For the Stroop test, we also compared reaction times for incongruent vs congruent items.

For comparisons of multimodal MRI parameters, a simple 2-stage model was applied to differently spaced time points. Postoperative MRI scans were categorized according to the interval from the most recent surgery as follows: 1 to 2 yr (n = 25, 12 to 24 ± 2 mo) and 2 to 4 yr (n = 14, 30 to 48 ± 2 mo). Baseline longitudinal MPRAGE and diffusion images were compared with images obtained at both follow-up times. A subset of 18 patients recruited after January 2013 underwent rs-fMRI, enabling a comparison between the data obtained at baseline and those obtained at the 1- to 2-yr follow-up. Changes in neuroimaging parameters extracted from ROI-based analysis were evaluated using paired *t*-tests, corrected for multiple comparisons using the false discovery rate (FDR). To explore relationships between imaging parameters and neurobehavioral alterations, Pearson's product–moment correlation coefficient analysis was applied to neuroimaging parameters extracted from ROI-based analysis and alterations in neurobehavioral performance scores. A level of $P < .05$ was considered statistically significant. All statistical analyses were performed using R (R Core Team (2013). R: A language and environment for statistical computing. R Foundation for Statistical Computing, Vienna, Austria. URL http://www.R-project.org/.).

TABLE 1. Patient Characteristics

Age			37.6 ± 9.7
F/M			20/5
Clinical presentations			
		Headache	5
		Hemorrhage	6
		TIA	12
		Minor stroke	2
Preoperative FIQ			94.4 ± 19.5 (range 57-124)
		Headache	80.8 ± 14.4
		Hemorrhage	101.5 ± 16.2
		TIA	91.0 ± 18.3
		Minor stroke	93.0 ± 16.7
Revascularization surgery			
		Unilateral	9
		Bilateral	16
Neovascularization hemisphere (percentage)			
	Direct bypass	Good	26 (63.4%)
		Fair	13 (31.7%)
		Poor	2 (4.9%)
	Indirect bypass	Good	10 (24.4%)
		Fair	18 (43.9%)
		Poor	13(31.7%)

RESULTS

Patient Characteristics

Patient characteristics are summarized in Table 1. Preoperative mean intelligence scores were within the normal range (mean FIQ: 94.4 ± 19.5; range: 57-124). Preoperative evaluations of frontal lobe function revealed abnormalities beyond one standard deviation from the norm in 3 patients (12%) on the TMT-A, 1 patient (4%) on the TMT-B, 6 patients (24%) on the WCST, and 6 patients (24%) on the Stroop test. Postoperative magnetic resonance angiography revealed favorable revascularization in all but one treated hemisphere (patency of direct bypass: 95%, effective indirect bypass: 69%, respectively).[18] Eight professional workers were able to return to the same work postsurgery. Two college students were able to resume school postsurgery.

Neuropsychological Examinations

The results of the cognitive function tests are summarized in Table 2. Significant increases in FIQ, PIQ, PO, and PS scores on the WAIS-III were observed between the preoperative and

TABLE 2. Results of Neurocognitive Examinations

Examinations	Measurements	Pre Average	SD	Post Average	SD	*P* value 2-tail
WAIS-III (n = 22)	VIQ	90.4	(15.8)	90.8	(17.6)	.753
	PIQ	92.2	(16.3)	98.2	(17.3)	**.006**
	FIQ	90.6	(16.7)	93.7	(18.5)	.033
	VC	92.0	(16.8)	93.0	(18.3)	.402
	PO	94.2	(17.2)	98.6	(18.8)	**.030**
	WM	85.6	(15.6)	85.7	(15.6)	.725
	PS	90.1	(16.6)	96.4	(15.3)	**.002**
TMT (n = 21)	TMT-A (Z score)	0.47	(0.98)	0.49	(1.16)	.925
	TMT-B (Z score)	0.49	(0.89)	0.55	(0.89)	.478
WCST (n = 17)	CA	4.5	(1.7)	4.2	(1.9)	.652
	PEN	3.9	(4.8)	3.4	(3.4)	.489
	DMS	1.0	(1.0)	0.9	(1.2)	1.000
Stroop (n = 17)	Reaction time (s)	7.4	(5.8)	6.2	(3.6)	.078*
CPT (n = 12)	Reaction time (ms)	444.1	(115.1)	427.6	(83.6)	.478
WMS (n = 8)	Verbal memory	93.4	(14.3)	100.8	(15.4)	.064
	Visual memory	100.5	(18.1)	109.4	(10.2)	.084
	General memory	94.7	(16.7)	103.7	(14.9)	**.019**
	Attention	92.8	(17.7)	97.1	(12.0)	.259
	Delayed recall	90.8	(21.2)	105.3	(11.2)	**.016**

Bold letter indicates significant changes in paired t-test with $P < .05$.
*$P = .039$ in one-tail t-test.

postoperative periods ($P < .05$). Increases beyond the clinically meaningful threshold specified in the WAIS-III manual (see **Supplemental Digital Content 1**) were observed in 36.4, 31.8, 27.3, and 59.1% of patients for the PIQ, FIQ, PO, and PS components of the WAIS-III, respectively. A 1-tailed *t*-test revealed that reaction times on the Stroop test decreased following surgery ($P = .039$). Increases in the general memory and delayed recall scores on the WMS were also observed post- vs preoperatively ($P < .05$, 2-tailed).

Neuroimaging Analysis

Morphometric Alterations

Significant increases in the cerebrospinal fluid (CSF) space and white matter hypointensities were observed post- vs preoperatively (see **Table, Supplemental Digital Content 2**). Volume increases were observed in the lateral and third ventricles, and in the CSF ($P < .05$, FDR corrected; Figure 1). Volume reductions were identified in corpus callosum, subcortical gray matter nuclei, and in remote white matter areas including the cerebellar hemisphere ($P < .05$, FDR corrected, Figure 1). Comparisons between baseline and the 2- to 4-yr follow-up revealed a trend of localized cortical thinning in the inferior and middle frontal gyri ($P < .05$, uncorrected; see **Figure, Supplemental Digital Content 3**).

White Matter Microstructural Alterations

Voxel-based analyses did not reveal any significant alterations in FA or MD between baseline and the 1- to 2-yr follow-up. However, ROI-based analyses (baseline vs 1-2 yr) revealed increases in MD in the corpus callosum ($P < .05$, FDR corrected). Voxel-based analyses also revealed significant increases in FA and decreases in MD in multiple white matter tracts between baseline and the 2- to 4-yr follow-up ($P < .05$ for all, TFCE corrected; Figure 2). Areas identified in voxel-based analyses were distributed in portions of the anterior internal capsule, superior corona radiata, posterior thalamic radiation, inferior occipitofrontal fasciculus, and superior longitudinal fasciculus (SLF). ROI-based analyses revealed a significant increase in FA in the bilateral SLF between baseline and the 2- to 4-yr follow-up (right: $P = .001$, FDR corrected; left: $P = .006$, FDR corrected; Figure 2). The results of the ROI-based analyses are summarized in **Tables and Figures, Supplemental Digital Content 2–4**.

Alterations in Resting Brain Connectivity

The ROI–ROI functional connectivity was increased in 20 connected units post- vs preoperatively (Table 3). Significant increases were observed predominantly in the cerebro-cerebellar circuit between the prefrontal regions (inferior frontal gyrus, medial frontal gyrus, superior medial frontal area) and cerebellum (cerebellar hemisphere, vermis; $P < .05$, FDR corrected; Figure 3). Among these 20 regions exhibiting significant increases, 67.7% (14 pairs of units) belonged to the prefrontal regions. This percentage was significantly higher than the expected rate of 25.9%, given 30 prefrontal regions among a total of 116 regions ($P < .001$; see **Table, Supplemental Digital Content 5**).

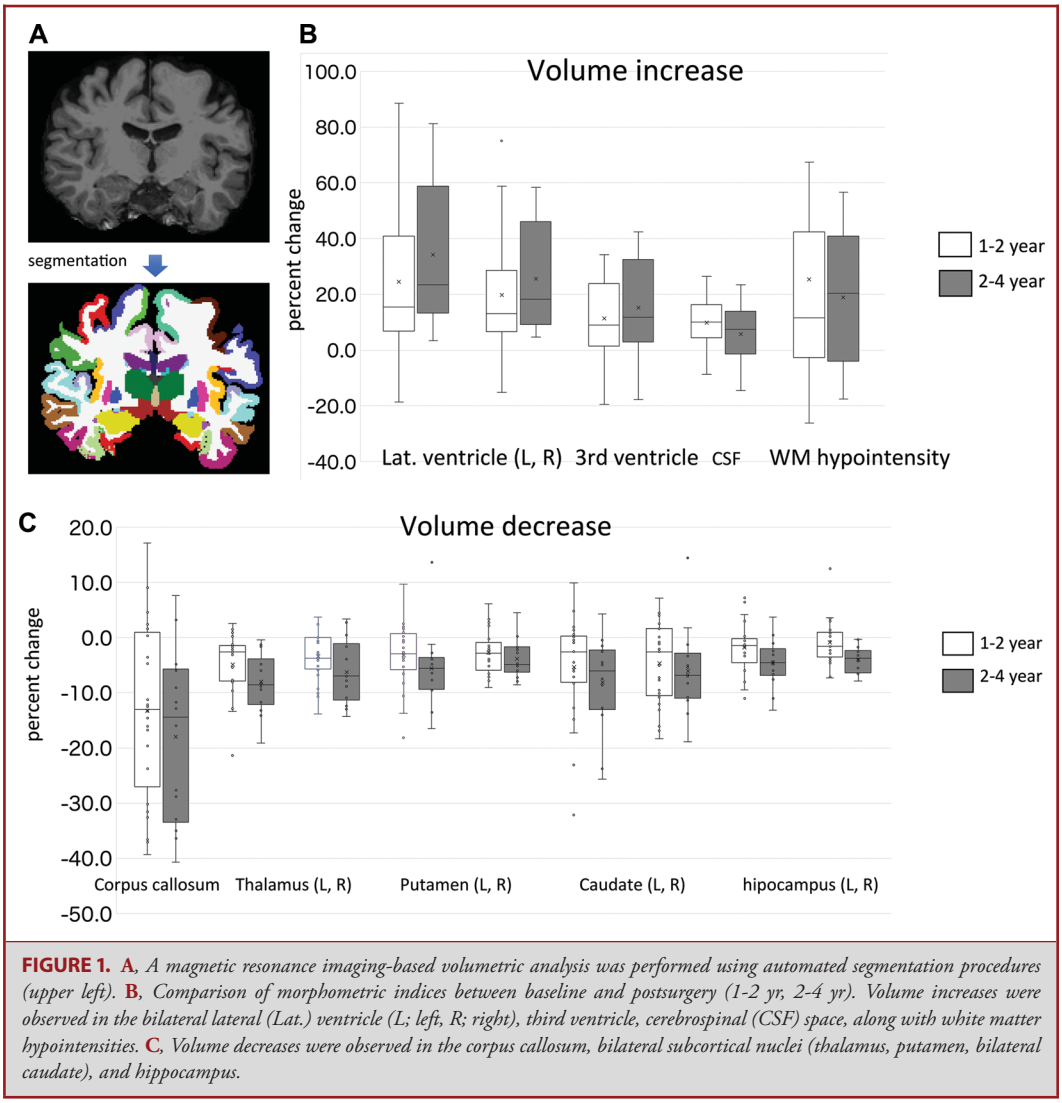

FIGURE 1. **A**, *A magnetic resonance imaging-based volumetric analysis was performed using automated segmentation procedures (upper left).* **B**, *Comparison of morphometric indices between baseline and postsurgery (1-2 yr, 2-4 yr). Volume increases were observed in the bilateral lateral (Lat.) ventricle (L; left, R; right), third ventricle, cerebrospinal (CSF) space, along with white matter hypointensities.* **C**, *Volume decreases were observed in the corpus callosum, bilateral subcortical nuclei (thalamus, putamen, bilateral caudate), and hippocampus.*

Correlation Analysis

We investigated the relationships among changes in neuropsychological test scores, age, clinical presentation, type of surgery (unilateral vs bilateral), preoperative rCBF, morphometric/diffusion properties, and resting brain connectivity. Pre- and postoperative changes in neuropsychological test scores (PIQ, FIQ, PO, PS) and Stroop test reaction times were used as indices of cognitive improvement. Resting brain connectivity was positively correlated with changes in PIQ, FIQ, and PO in the Cerebellum9R-Superior medial frontal gyrus_R unit (PIQ: $r[15] = 0.73$, $P < .001$; FIQ: $r[15] = 0.50$, $P = .041$; PO: $r[15] = 0.52$, $P = .043$; Figure 3). We observed a significant positive correlation between rCBF in the left medial frontal region and changes in PIQ ($r[20] = 0.55$, $P = .008$), FIQ ($r[20] = 0.54$, $P = .010$) and PS ($r[19] = 0.44$, $P = .046$), suggesting that changes in preoperative rCBF in the medial frontal lobe are associated with improvements in intellectual ability (Figure 4). Preoperative rCBF in the left parietal region also exhibited a significant positive correlation with improvements PIQ ($r[20] = 0.44$, $P = .038$) and PO ($r[19] = 0.46$, $P = .035$; Figure 4).

DISCUSSION

In the present study, we investigated structural and functional changes following revascularization surgery in patients with MMD. Alterations in cognitive test scores suggested that patients experienced improvements in spatial information processing and attention following revascularization surgery. Additionally, longitudinal morphometric analyses revealed mild ventricular

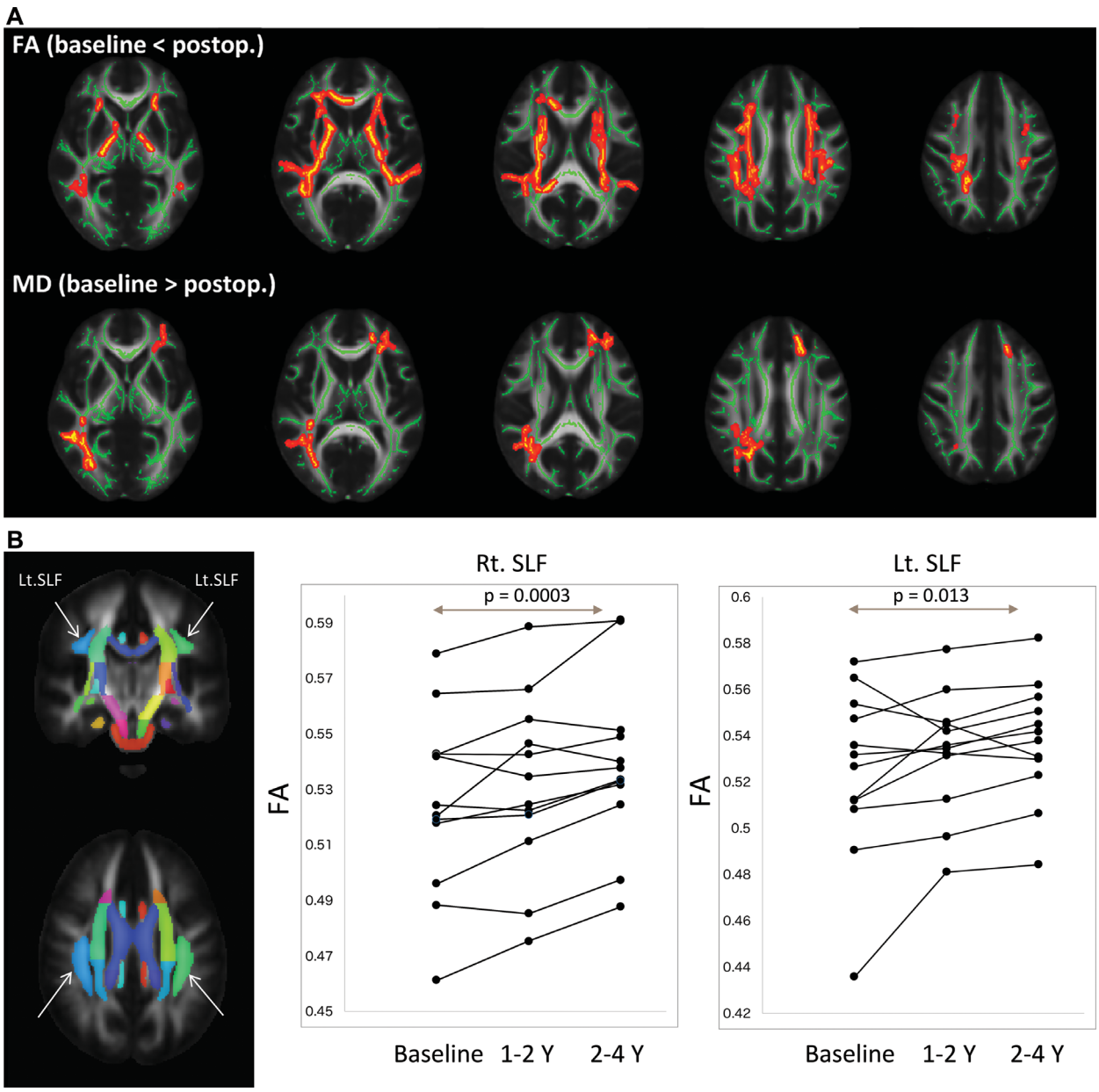

FIGURE 2. **A**, *A whole-brain voxel-based analysis of white matter using tract-based spatial statistics (TBSS) revealed postsurgical alterations in fractional anisotropy (FA) and mean diffusivity (MD). Voxels exhibiting significant increases in FA and decreases in MD are shown overlaid on the standardized FA maps (FMRIB58_FA) and FA skeleton (green) ($P < .05$, corrected by means of threshold-free cluster enhancement). Suprathreshold voxels were enlarged for illustrative purposes.* **B**, *A region of interest (ROI)-based analysis revealed gradual increases in FA in the bilateral superior longitudinal fasciculus (SLF), which reached statistical significance at 2 to 4 yr after surgery.*

enlargement, volume reductions in subcortical gray matter nuclei, and cortical thinning, suggestive of postoperative CSF retention and neuron loss. DTI revealed postoperative white matter reorganization, as indicated by increased FA and decreased MD. White matter alterations occurred in functionally important fiber tracts including the SLF, where parieto-frontal association areas are connected. Furthermore, increases in resting brain connectivity were identified in prefrontal-cerebellar circuits. Collectively, our results indicate that alterations in brain structure and function occur following revascularization surgery.

TABLE 3. Increase of Resting Brain Connectivity

Analysis unit	T-value	p-unc	p-FDR
Amygdala R-Insula L	5.96	0.000	0.002
Cerebelum 9 L-Frontal Sup R	5.15	0.000	0.007
Cerebelum 9 L-Frontal Sup Med R	4.94	0.000	0.007
Cerebelum 9 L-Frontal Sup Med L	4.34	0.000	0.017
Cingulum Mid L-Paracentral Lob R	4.6	0.000	0.029
Cerebelum 9 L-Frontal Mid R	3.94	0.001	0.030
Cerebelum 9 R-Frontal Mid R	4.21	0.001	0.046
Cerebelum 9 R-Frontal Sup Med R	3.94	0.001	0.046
Cerebelum 9 R-Heschl L	3.88	0.001	0.046
Frontal Med Orb R-Vermis 10	4.37	0.000	0.048

When comparing pre- and postsurgical measures of cognitive function, it is important to determine whether the observed differences are clinically meaningful.[19] Here, we attempted to mitigate learning effects by applying follow-up measurements a median of 18 mo after surgery. Our results suggested that patients exhibited clinically relevant increases in performance (IQ points changes >9) with regard to FIQ, PIQ, PO, and PS, while no remarkable changes in VIQ were observed. Patients also tended to exhibit improvement on the Stroop test, which reflects attention-related cognition. Our findings suggest that cognitive impairments are reversible in adult patients with MMD.

The effects of revascularization may differ based on the type of procedure. Combined direct/indirect bypass covers a wide

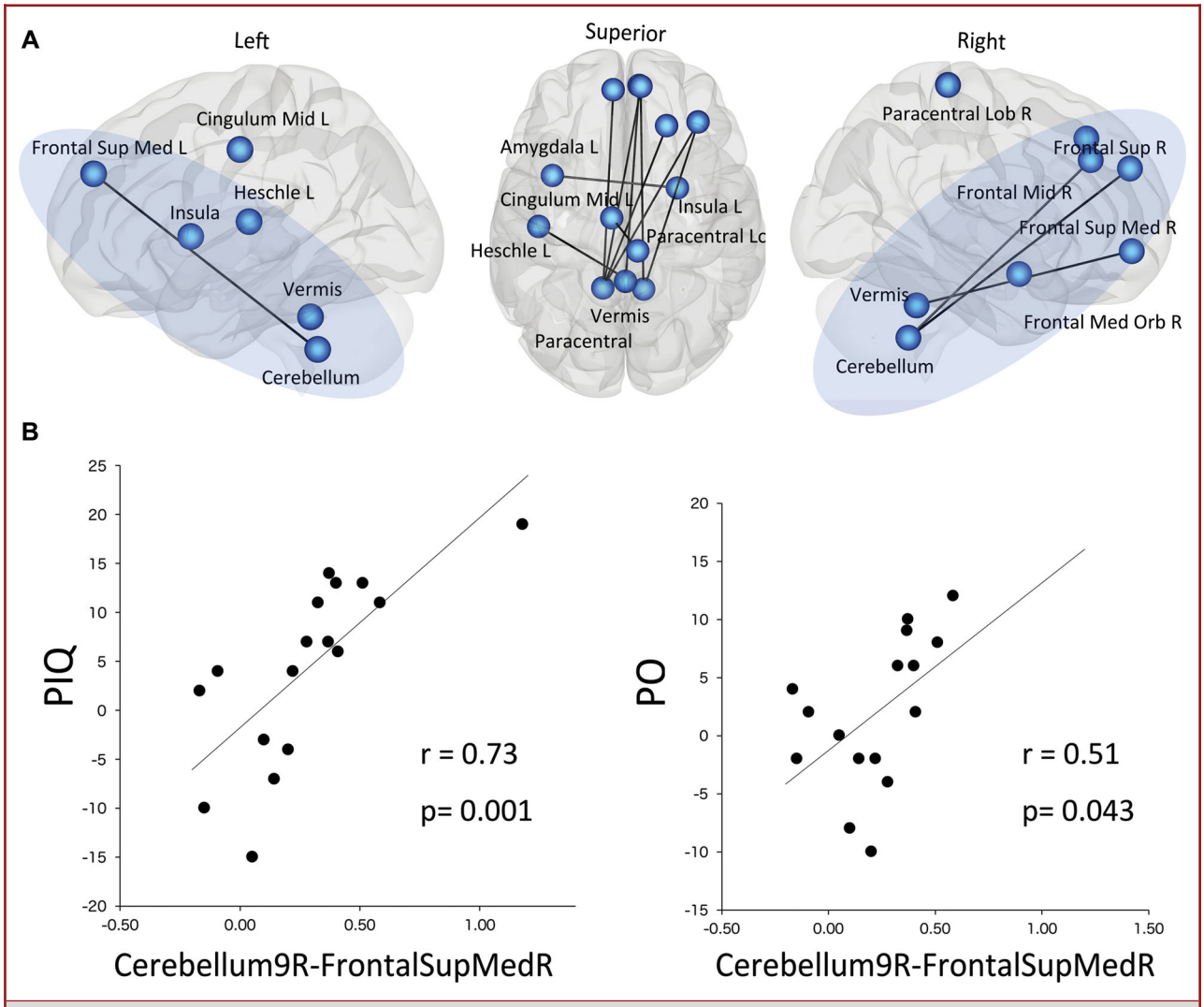

FIGURE 3. **A**, *Resting-state functional magnetic resonance imaging (rs-fMRI) analyses revealed postsurgical increases in resting brain connectivity, predominantly in cerebro-cellebellar units.* **B**, *The scatterplots show the relationship between connectivity indices and neuropsychological test performance. Significant positive correlations were observed between the Cerebellum9R-Superior medial frontal gyrus_R unit and changes in performance intelligence quotient (PIQ; $r = 0.73$, $P < .001$) and perceptual organization (PO; $r = 0.52$, $P = .043$), respectively.*

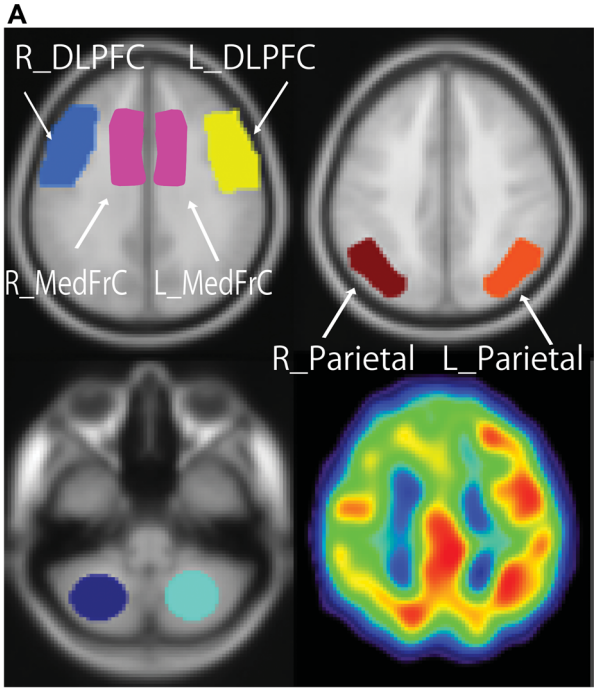

B

	L_DLPFC	R_DLPFC	L_MedFrC	R_MedFrC	L_Parietal	R_Parietal
PIQ	0.02	0.24	**0.61 ***	0.32	**0.43 ***	0.02
FIQ	-012	0.27	**0.54 ***	0.33	**0.44 ***	-0.20
PO	0.07	**0.40 ***	**0.44 ***	0.10	**0.46 ***	-0.07
PS	0.10	0.04	**0.45 ***	0.25	0.33	0.07
Stroop	0.10	-0.24	0.24	0.21	0.13	0.35

FIGURE 4. *Results of the correlation analysis between regional cerebral blood flow (rCBF) and changes in cognitive performance.* **A**, *Regions of interest (ROIs) included the left (L) and right (R) dorsolateral prefrontal cortex (DLPFC), medial frontal cortex (MedFrC), parietal cortex, and cerebellar hemisphere.* **B**, *In the correlation matrix, correlations with r values > 0.30 are indicated in bold, while significant correlations (at P < .05) are marked with an asterisk (∗). Significant correlations were observed between cognitive performance and rCBF in the left MedFrC and left parietal cortex.*

frontotemporal region, allowing for maximal neovascularization. In a certain population, indirect bypass takes over the territory perfused by direct bypass within 6 mo to 1 yr. Therefore, a 1-yr interval would be necessary to observe cognitive benefits.

Voxel-based brain morphometry using T1-MPRAGE permits the evaluation of gray/white matter structures. In the present study, we observed ventricular enlargement, reduced basal ganglia volume, and cortical thinning following revascularization surgery, suggestive of CSF retention, neuron loss, and remote effects due to subtle brain injury. CSF retention was likely associated with our extensive indirect procedure. Nevertheless, we consider this phenomenon to be benign, as no patients exhibited hydrocephalus signs. Volume reductions in the corpus callosum and subcortical gray matter subnuclei suggested transneuronal atrophy. In our study, the average patient age was 37.6 yr. At this age, the volumes of the corpus callosum and white matter FA have not yet begun to decrease.[20] Thus, it is unlikely that the changes we observed were due to age-related atrophy. Cerebral hyperperfusion may have also induced cortical thinning in the dorsolateral prefrontal cortex, as suggested previously.[21,22] We were unable to identify correlations between atrophy and changes in cognitive function. Therefore, we speculate that these findings represent radiological changes only, with little effect on the clinical results.

Nuclear medicine examinations are useful for diagnosing hemodynamic insufficiency and tracking changes in brain metabolism following surgery.[23] However, longitudinal applications are not feasible for routine clinical follow-up evaluations. Alternatively, multimodal MRI has enabled the examination of brain morphometry, white matter integrity, and connectivity among distant brain regions.[10,24,25] DTI detects alterations in brain white matter microstructure.[26] FA measures the degree to which the diffusion of water molecules is restricted by microstructural elements.[7] Reduced FA is considered to reflect decreases in the number of myelinated fibers and breakdown of the myelin sheath.[27,28] Previous studies have reported that patients with MMD exhibit reduced FA in normal-appearing white matter, suggestive of decreased white matter fiber density due to ischemic injury.[24,29] In our study, we observed increased FA in multiple white matter tracts, suggesting that white matter reorganization occurred during the postoperative period. Among the areas exhibiting such increases, the SLF is known to mediate information transfer by connecting the parieto-frontal association areas. White matter reorganization following cerebral revascularization has also been reported among patients who have undergone carotid endoarterectomy.[30]

Several recent studies have utilized rs-fMRI to investigate cerebrovascular diseases, including MMD.[10,25,31,32] Changes in low-frequency BOLD signals across distant brain regions, which reflect spontaneous brain activity, are used as an index of functional connectivity.[33] Brain regions exhibiting synchronized low-frequency BOLD fluctuations are called resting-state networks.[9] In MMD, the relationships among BOLD signal fluctuations are disrupted predominantly in regions belonging to resting-state networks.[31,32] In the present study, significant alterations in connectivity were observed in the unit including the prefrontal region and cerebellum. A previous study reported that this unit differed most significantly between patients and controls.[32] Furthermore, the anatomical pattern suggests an association with crossed cerebellar diaschisis.[34]

We observed a significant positive correlation between preoperative rCBF in the left medial frontal region and changes in PIQ and PS. The medial frontal lobe is associated with attention.[35] Thus, preoperative rCBF in the medial frontal lobe may be associated with preserved tissue integrity in this region, impairments in which may interfere with accomplishing simple

tasks quickly. Preoperative rCBF in the left parietal region was also significantly positively correlated with improvements in PIQ and PO. The parietal region is associated with visual information processing, consistent with the observed improvements in PO.[36]

Limitations

The present study has some strengths and limitations. As a strength, we designed this study in a manner that observer bias is free. To achieve this, we used a universal ROI atlas that can be applied to images normalized to a standardized template (MNI template in this study). In addition, all image processing steps were performed semi-automatically, using the parameters mentioned in the "Methods" sectionso as to allow reproducibility. This procedure reduces the confounding effects from interindividual morphological variability and is sensitive to the changes that are associated with longitudinal study design.[15] Another strength of this study is maintaining quality assurance throughout the study period. The results of this study can be affected by variation in magnetic homogeneity and the appearance of artifacts between the MRI scans. We attempted to limit this possibility by daily quality assurance tests that check any remarkable variation in magnetic field homogeneity, coil sensitivity profile, and appearance of artifacts. Furthermore, the results in the present study can be applied for the patients treated with combined direct/direct bypass such as in our case series. As a limitation, the number of patients who underwent neuroimaging 2 to 4 yr after surgery was insufficient to reach a definitive conclusion regarding the DTI study. Next, the present study included patients with multiple clinical modes of onset, which may have influenced cognitive outcomes. In addition, the neurocognitive examinations utilized in our study are unlikely to cover the full spectrum of cognitive changes. Lastly, we did not investigate CBF using single-photon emission computed tomography at >1 yr after surgery, as such examinations are considered invasive for stable patients. Several institutions implement rCBF within 1 wk after surgery, but the data are strongly affected by the postoperative hyperperfusion phenomenon, reduced brain metabolism after craniotomy, and cerebral ischemia. We consider not to use the rCBF data taken within 1wk after surgery to evaluate the outcome of the neovascularization. Alterations in tissue perfusion may thus be a major contributor to cognitive improvement.

CONCLUSION

Revascularization surgery may improve processing speed and attention in adult patients with MMD. Moreover, multimodal MRI may be used to detect subtle postsurgical brain structural changes, reorganization of white matter tracts, and brain connectivity alterations.

Disclosures

This study was supported by a grant from the Research Committee on Moyamoya Disease, sponsored by the Ministry of Health, Labor, and Welfare of Japan. The authors have no personal, financial, or institutional interest in any of the drugs, materials, or devices described in this article.

REFERENCES

1. Kuroda S, Houkin K. Moyamoya disease: Current concepts and future perspectives. *Lancet Neurol*. 2008;7(11):1056-1066.
2. Fang L, Huang J, Zhang Q, Chan RC, Wang R, Wan W. Different aspects of dysexecutive syndrome in patients with moyamoya disease and its clinical subtypes. *J Neurosurg*. 2016;125(2):299-307.
3. Festa JR, Schwarz LR, Pliskin N, et al. Neurocognitive dysfunction in adult moyamoya disease. *J Neurol*. 2010;257(5):806-815.
4. Karzmark P, Zeifert PD, Bell-Stephens TE, Steinberg GK, Dorfman LJ. Neurocognitive impairment in adults with moyamoya disease without stroke. *Neurosurgery*. 2012;70(3):634-638.
5. Miyamoto S, Yoshimoto T, Hashimoto N, et al.. Effects of extracranial-intracranial bypass for patients with hemorrhagic moyamoya disease: results of the Japan adult moyamoya trial. *Stroke*. 2014;45(5):1415-1421.
6. Zeifert PD, Karzmark P, Bell-Stephens TE, Steinberg GK, Dorfman LJ. Neurocognitive performance after cerebral revascularization in adult moyamoya disease: results of the Japan adult moyamoya trial. *Stroke*. 2017;48(6):1514-1517.
7. Beaulieu C. The basis of anisotropic water diffusion in the nervous system - a technical review. *NMR Biomed*. 2002;15(7-8):435-455.
8. Biswal B, Yetkin FZ, Haughton VM, Hyde JS. Functional connectivity in the motor cortex of resting human brain using echo-planar MRI. *Magn Reson Med*. 1995;34(4):537-541.
9. Greicius MD, Krasnow B, Reiss AL, Menon V. Functional connectivity in the resting brain: a network analysis of the default mode hypothesis. *Proc Natl Acad Sci USA*. 2003;100(1):253-258.
10. Lei Y, Li YJ, Guo QH, et al. Postoperative executive function in adult moyamoya disease: a preliminary study of its functional anatomy and behavioral correlates. *J Neurosurg*. 2017;126(2):527-536.
11. Houkin K, Kamiyama H, Takahashi A, Kuroda S, Abe H. Combined revascularization surgery for childhood moyamoya disease: STA-MCA and encephalo-duro-arterio-myo-synangiosis. *Child's Nerv Syst*. 1997;13(1):24-29.
12. Kuroda S, Houkin K. Bypass surgery for moyamoya disease: concept and essence of sugical techniques. *Neurol Med Chir(Tokyo)*. 2012;52(5):287-294.
13. Maldjian JA, Laurienti PJ, Burdette JH. Precentral gyrus discrepancy in electronic versions of the Talairach atlas. *Neuroimage*. 2004;21(1):450-455.
14. Dale AM, Fischl B, Sereno MI. Cortical surface-based analysis. I. Segmentation and surface reconstruction. *Neuroimage*. 1999;9(2):179-194.
15. Reuter M, Schmansky NJ, Rosas HD, Fischl B. Within-subject template estimation for unbiased longitudinal image analysis. *Neuroimage*. 2012;61(4):1402-1418.
16. Tabesh A, Jensen JH, Ardekani BA, Helpern JA. Estimation of tensors and tensor-derived measures in diffusional kurtosis imaging. *Magn Reson Med*. 2011;65(3):823-836.
17. Wakana S, Jiang H, Nagae-Poetscher LM, van Zijl PC, Mori S. Fiber tract-based atlas of human white matter anatomy. *Radiology*. 2004;230(1):77-87.
18. Uchino H, Kim JH, Fujima N, et al. Synergistic interactions between direct and indirect bypasses in combined procedures: the significance of indirect bypasses in moyamoya disease. *Neurosurgery*. 2017;80(2):201-209.
19. Miyoshi K, Chida K, Kobayashi M, et al. Two-year clinical, cerebral hemodynamic, and cognitive outcomes of adult patients undergoing medication alone for symptomatically ischemic moyamoya disease without cerebral misery perfusion: a prospective cohort study. *Neurosurgery*. 2019;84(6):1233-1241.
20. Prendergast DM, Ardekani B, Ikuta T, et al. Age and sex effects on corpus callosum morphology across the lifespan. *Hum Brain Mapp*. 2015;36(7):2691-2702.
21. Kazumata K, Tha KK, Uchino H, et al. Topographic changes in cerebral blood flow and reduced white matter integrity in the first 2 weeks following revascularization surgery in adult moyamoya disease. *J Neurosurg*. 2017;127(2):260-269.
22. Kazumata K, Uchino H, Tokairin K, et al. Cerebral hyperperfusion syndrome after revascularization surgery in moyamoya disease: region-symptom mapping and estimating a critical threshold. *World Neurosurg*. 2018;114:e388-e395.
23. Kuroda S, Kashiwazaki D, Hirata K, Shiga T, Houkin K, Tamaki N. Effects of surgical revascularization on cerebral oxygen metabolism in patients with moyamoya disease: an 15O-gas positron emission tomographic study. *Stroke*. 2014;45(9):2717-2721.

24. Kazumata K, Tha KK, Narita H, et al. Chronic ischemia alters brain microstructural integrity and cognitive performance in adult moyamoya disease. *Stroke*. 2015;46(2):354-360.
25. Lei Y, Li Y, Ni W, et al. Spontaneous brain activity in adult patients with moyamoya disease: a resting-state fMRI study. *Brain Res*. 2014;1546(1872-6240 (Electronic)):27-33.
26. Le Bihan D. Apparent diffusion coefficient and beyond: What diffusion MR imaging can tell us about tissue structure. *Radiology*. 2013;268(2):318-322.
27. Sullivan EV, Pfefferbaum A. Diffusion tensor imaging and aging. *Neurosci Biobehav Rev*. 2006;30(6):749-761.
28. Bartzokis G, Sultzer D, Lu PH, Nuechterlein KH, Mintz J, Cummings JL. Heterogeneous age-related breakdown of white matter structural integrity: implications for cortical "disconnection" in aging and Alzheimer's disease. *Neurobiol Aging*. 2004;25(7):843-851.
29. Kazumata K, Tha KK, Narita H, et al. Characteristics of diffusional kurtosis in chronic ischemia of adult moyamoya disease: comparing diffusional kurtosis and diffusion tensor imaging. *Am J Neuroradiol*. 2016;37(8):1432-1439.
30. Sato Y, Ito K, Ogasawara K, et al. Postoperative increase in cerebral white matter fractional anisotropy on diffusion tensor magnetic resonance imaging is associated with cognitive improvement after uncomplicated carotid endarterectomy: tract-based spatial statistics analysis. *Neurosurgery*. 2013;73(4):592-599; discussion 598–599.
31. Lei Y, Su J, Jiang H, et al. Aberrant regional homogeneity of resting-state executive control, default mode, and salience networks in adult patients with moyamoya disease. *Brain Imaging Behav*. 2017;11(1):176-184.
32. Kazumata K, Tha KK, Uchino H, Ito M, Nakayama N, Abumiya T. Mapping altered brain connectivity and its clinical associations in adult moyamoya disease: a resting-state functional MRI study. *PLoS One*. 2017;12(8):e0182759.
33. Biswal BB, Van Kylen J, Hyde JS. Simultaneous assessment of flow and BOLD signals in resting-state functional connectivity maps. *NMR Biomed*. 1997;10(4-5):165-170.
34. Baron JC BM, Comar D, Castaigne P. "Crossed cerebellar diaschisis" in human supratentorial brain infarction. *Trans Am Neurol Assoc*. 1981;105(0065-9479 (Print)):459-461.
35. Posner MI, Rothbart MK, Voelker P. Developing brain networks of attention. *Curr Opin Pediatr*. 2016;28(6):720-724.
36. Bartolomeo P, Thiebaut de Schotten M, Chica AB. Brain networks of visuospatial attention and their disruption in visual neglect. *Front Hum Neurosci*. 2012;6:110.

Supplemental digital content *is available for this article at www.neurosurgeryonline.com.*

Supplemental Digital Content 1. The Supplemental Digital Content expands on the Methods provided. Surgical strategy; The MRI parameters; Postprocessing methods for multimodal MRI data; Cognitive assessments; Threshold of meaningful increase in the WAIS-III.

Supplemental digital content 2. Table. Changes of global index in volume measurements.

Supplemental Digital Content 3. Figure. Changes in the cortical thickness.

Supplemental Digital Content 4. Table. Changes of diffusion index.

Supplemental Digital Content 5. Table. Increase of resting brain connectivity.